Process Biochemistry 44 (2009) 1315–1322

Contents lists available at ScienceDirect

Process Biochemistry

journal homepage: www.elsevier.com/locate/procbio

Process for biological oxidation and control of dissolved iron in bioleach liquors

P. Nurmi [a,*], B. Özkaya [a,1], A.H. Kaksonen [a,2], O.H. Tuovinen [a,b], M.-L. Riekkola-Vanhanen [c], J.A. Puhakka [a]

[a] Department of Chemistry and Bioengineering, Tampere University of Technology, P.O. Box 541, FI-33101 Tampere, Finland
[b] Department of Microbiology, Ohio State University, 484 West 12th Avenue, Columbus, OH 43210, USA
[c] Talvivaara Mining Company Plc., Ahventie 4 B 47, FI-02170 Espoo, Finland

ARTICLE INFO

Article history:
Received 27 January 2009
Received in revised form 9 July 2009
Accepted 10 July 2009

Keywords:
Bioleaching
Ferric iron regeneration
Iron oxidation
Iron precipitation
Iron control
Leptospirillum ferriphilum

ABSTRACT

Iron has a central role in bioleaching and biooxidation processes. Fe^{2+} produced in the dissolution of sulfidic minerals is re-oxidized to Fe^{3+} mostly by biological action in acid bioleaching processes. To control the concentration of iron in solution, it is important to precipitate the excess as part of the process circuit. In this study, a bioprocess was developed based on a fluidized-bed reactor (FBR) for Fe^{2+} oxidation coupled with a gravity settler for precipitative removal of ferric iron. Biological iron oxidation and partial removal of iron by precipitation from a barren heap leaching solution was optimized in relation to the performance and retention time (τ_{FBR}) of the FBR. The biofilm in the FBR was dominated by *Leptospirillum ferriphilum* and "*Ferromicrobium acidiphilum*." The FBR was operated at pH 2.0 ± 0.2 and at 37 °C. The feed was a barren leach solution following metal recovery, with all iron in the ferrous form. 98–99% of the Fe^{2+} in the barren heap leaching solution was oxidized in the FBR at loading rates below 10 g Fe^{2+}/L h (τ_{FBR} of 1 h). The optimal performance with the oxidation rate of 8.2 g Fe^{2+}/L h was achieved at τ_{FBR} of 1 h. Below the τ_{FBR} of 1 h the oxygen mass transfer from air to liquid limited the iron oxidation rate. The precipitation of ferric iron ranged from 5% to 40%. The concurrent Fe^{2+} oxidation and partial precipitative iron removal was maximized at τ_{FBR} of 1.5 h, with Fe^{2+} oxidation rate of 5.1 g Fe^{2+}/L h and Fe^{3+} precipitation rate of 25 mg Fe^{3+}/L h, which corresponded to 37% iron removal. The precipitates had good settling properties as indicated by the sludge volume indices of 3–15 mL/g but this step needs additional characterization of the properties of the solids and optimization to maximize the precipitation and to manage sludge disposal.

1. Introduction

Ferric iron is the key oxidant in biohydrometallurgical processes where sulfide minerals such as pyrite (FeS_2), pyrrhotite ($Fe_{1-x}S$), covellite (CuS) and sphalerite (ZnS) are oxidized. One of the main mechanisms of bacterial catalysis in the dissolution of sulfide minerals is based on the biological oxidation of ferrous iron with oxygen as the electron acceptor [1]. Fe^{3+} thus produced chemically oxidizes sulfide minerals and is reduced in this redox reaction to Fe^{2+}. Iron re-oxidation is essential in the bioleaching process because Fe^{3+} is an important electron shuttle and a chemical oxidant. Recirculation of Fe^{3+} and Fe^{2+} containing leach solutions back to the process is common practice but leads to the accumulation of high concentrations of dissolved iron [2–4]. Fe^{2+} can be oxidized chemically in acid solutions, but microbial oxidation occurs 10^5–10^6 times faster compared to the chemical oxidation [5].

Various types of bioreactors, including fluidized-beds, packed-beds, trickle-beds, circulating-beds, agitated reactors and rotating biological contactors, have been tested for their potential for high-rate ferrous iron oxidation by acidophilic microorganisms. These reactor types and their performances are compared in Table 1. The tendency of iron-oxidizing microorganisms to grow on surfaces has been exploited in bioreactors with various cell immobilization matrices, thereby effectively ensuring high and stable biomass retention. The highest iron oxidation rates have been achieved in packed-bed and fluidized-bed bioreactors with granular activated carbon as the best support material [19,20].

In addition to abundant Fe-sulfides, common Cu-, Zn-, and Ni-sulfide minerals such as sphalerite, chalcopyrite ($CuFeS_2$), and pentlandite ($(Fe,Ni)_9S_8$) contain iron, and their acid leaching leads to the accumulation of iron in leach liquors. Accumulation of iron may result in adverse effects on the bioleaching due to iron precipitation on mineral surfaces, pipelines and orifices and toxicity of high iron concentrations to microorganisms. Biological iron oxidation has been studied in detail. There is, however, a very

* Corresponding author. Present address: MTT Agrifood Research Finland, Biotechnology and Food Research, FI-31600 Jokioinen, Finland.
Tel.: +358 50 351 8211.
E-mail address: pauliina.nurmi@inbox.com (P. Nurmi).
[1] Present address: Department of Environmental Engineering, Faculty of Civil Engineering, Davutpasa Campus, Yildiz Technical University, TR-34342 Istanbul, Turkey.
[2] Present address: CSIRO Land and Water, Underwood Avenue, Floreat, WA 6014, Australia.

1359-5113/$ – see front matter © 2009 Elsevier Ltd. All rights reserved.
doi:10.1016/j.procbio.2009.07.004

Table 1
Biological iron oxidation rates achieved in various bioreactor configurations.

Reactor type	Support matrix	pH	Temperature (°C)	Aeration using	Maximum iron oxidation rate (g Fe^{2+}/L h)	Nature of precipitates (if any), other comments concerning precipitation	Reference
Fluidized-bed	Activated carbon	2.1 ± 0.2	37 ± 1	Air	8.2	Jarosites[a]	This study
Fluidized-bed	Activated carbon and jarosites	1.4 ± 0.1	37 ± 1	0.5% CO_2/ 99.5% O_2	26.4	Jarosites	[4]
Fluidized-bed	Activated carbon and jarosites	1.4 ± 0.1	37 ± 1	Air	6.9	Jarosites	[4]
Fluidized-bed	Activated carbon	1.35–1.5	23	Air	0.9	Jarosite, amount of precipitation was negligible, no problems of clogging	[6]
Flooded packed-bed	Siliceous stone	1.25	31	Air	11.25	Not mentioned	[7]
Inverse fluidized-bed	Activated carbon felt	1.05	40	Air	0.9	Not mentioned	[8]
Packed-bed	Expanded polystyrene	2.3	25	Air	0.72	Not mentioned	[9]
Packed-bed	Nickel alloy fiber	1.8	30	Air	20	N.d., extensive precipitation had a detrimental effect on iron oxidation rate and oxygen mass transfer rate to the medium	[10]
Packed-bed	Glass beads	1.35–1.5	23	Air	8.1	Jarosite, amount of precipitation was negligible, no problems of clogging	[6]
Packed-bed	Resin beads	1.35–1.5	23	Air	29.3	Jarosite, amount of precipitation was negligible, no problems of clogging	[6]
Packed-bed	Activated carbon	1.35–1.5	23	Air	52	Jarosite, amount of precipitation was negligible, no problems of clogging	[6]
Packed-bed	Poly(vinyl alcohol) gryogel	1.7	31	Air	3.1	N.d., above 95% of the initial iron was found to be in solution	[11]
Packed-bed	Polyurethane foam	1.7	30	Air	34.3	Not mentioned	[12]
Packed-bed	Quartz sand	2	20	Not mentioned	0.33	Not mentioned	[13]
Rotating biological contactor	Polyvinyl chloride	1.5–2.6	10–40	–	0.80	N.d., solid films of ferric iron developed on disk surfaces, maximum iron precipitation was around 9 g/day	[14]
Rotating biological contactor	Polyvinyl chloride	2.0–2.5	18	–	1.4	Not mentioned	[15]
Circulating-bed	Polyurethane foam	2.3	28	Air	1.56	N.d., 64% of initial total iron precipitated and mainly accumulated inside the support particles	[16]
Trickle-bed	Polyurethane foam	2.3	28–30	Air	4.4	Jarosites[b], extensive precipitation had a detrimental effect on iron oxidation rate	[17]
Airlift	Basalt, ferric iron precipitates	0–1.8	30	Air	8.1	N.d., initially used basalt was slowly removed and the ferric iron precipitates formed served as a biofilm carrier, these precipitates had highly suitable characteristics as a carrier material	[18]

N.d., not determined.
[a] Precipitates characterized by X-ray diffraction analysis (unpublished results).
[b] Solid phase analysis not performed.

limited amount of published information on simultaneous iron biooxidation and precipitation/removal processes and they are rarely reported in sufficient detail. Integration of these processes is essential for treatment of leach liquors since the concentration of dissolved iron must be controlled for successful leaching. A key process is the oxidation of ferrous iron in leach liquor for subsequent precipitation of Fe(III). In the present study, acidophilic bacteria were employed to oxidize ferrous iron in a bioprocess that involved a fluidized-bed reactor (FBR) coupled with a gravity settler. The specific objective of the study was to characterize the performance of bacterial oxidation of ferrous iron in an FBR which was integrated with partial precipitation of ferric iron in a gravity settler. The feed solution for the bioprocess was a barren heap leaching solution which had been treated for the recovery of valuable metals. Potential application of this process is for re-oxidation of dissolved iron in leach solution circuits followed by partial precipitative removal of ferric iron.

2. Materials and methods

2.1. Reactor setup

An FBR based system (Fig. 1) with granular activated carbon (Calgon Carbon Filtrasorb 200) as biomass carrier was used for the experiments at 37 °C. Sufficient liquid volume was maintained above the fluidized-bed to prevent the discharge of activated carbon particles from the FBR. The total working volume and the fluidized-bed volume of the FBR were 500 and 340 mL, respectively. The bed expansion or fluidization ratio was adjusted to 30% with sufficient upward velocity of the fluid. Before the current experiments, the FBR was fed for 80 days at 37 °C with simulated multimetal ore bioheap leaching solution from which Cu, Zn, Ni and Co had been removed [21]. In the current experiments the FBR was fed with a barren heap leaching solution obtained from a multimetal heap bioleaching pilot plant at Talvivaara, Finland, retrieved after the recovery of target metals. This solution was supplemented with a mineral salts medium containing (g/L) $(NH_4)_2HPO_4$ (0.35),

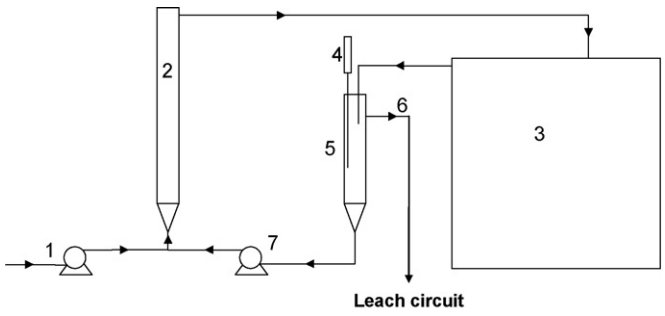

Fig. 1. Schematic diagram of the fluidized-bed reactor (FBR) system used for iron oxidation. (1) feed pump, (2) FBR, (3) settling tank, (4) aeration pump, (5) aeration unit, (6) final system effluent, (7) recycle pump. Not drawn to the scale. The settling tank had no special configuration to prevent discharge of the precipitates with the effluent.

Table 2
Performance of the integrated reactor system at different τ_{FBR} values.

τ_{FBR} (h)	Duration of the exp. (days)	Flow rate of feed pump (mL/h)	pH[a]	Fe^{2+} concentration in the FBR outlet (mg/L)	R_{FBR} (g/L h[a])	Fe^{2+} oxidation efficiency (%[a])	Fe^{3+} loading rate to the settling tank = R_{tot} (mg/L h[a])	Fe^{3+} precipitation rate (mg/L h[a])	Fe^{3+} precipitation efficiency (%[a])
5.0	12	68.0	1.8	130–140	1.5	98.3	20	N.d.	N.d.
2.5	10	136	1.9	80–140	3.2	98.7	41	1.4	3.2
1.5	12	227	2.1	50–60	5.2	99.3	69	11	16
1.0	10	339	2.0	50–80	8.2	99.2	110	26	20
0.7	7	485	2.2	60–2500	9.9	85.9	130	25	22
1.5	20	227	2.2	50–100	5.1	99.2	66	25	37
5.0	36	68.0	2.0	50–60	1.6	99.3	21	8.1	39

N.d., not determined.
[a] Average values.

K_2CO_3 (0.05) and $MgSO_4$ (0.05). The feed solution contained (mg/L) Fe (7900 ± 900), S (15800 ± 600), Na (1000 ± 50), K (20 ± 0), Mg (3800 ± 150), Mn (1450 ± 60), Ca (470 ± 10), Al (35 ± 5), Cu (1 ± 0), Zn (20 ± 0), Ni (90 ± 0) and Co (2 ± 0), all analyzed by ICP. All the iron in the feed was in the form of Fe^{2+}. The pH and the redox potential of the feed solution varied from 2.8 to 3.7 and from 140 to 230 mV (Ag/AgCl as the reference electrode), respectively. The performance of the FBR was characterized at retention times between 0.7 and 5 h. The retention time of the FBR (τ_{FBR}) refers to the theoretical hydraulic retention time of the feed solution in the fluidized-bed:

$$\tau_{FBR}(h) = \frac{V_{FBR}}{Q_f}$$

where V_{FBR} = fluidized-bed volume of the FBR (L) and Q_f = feed flow rate (L/h). The flow rates of the feed pump at the five different retention times tested in the FBR are summarized in Table 2.

The sampling point was the exit point of the FBR. Samples were taken daily or every second day. Following the oxidation in the FBR and the gravity settling, the treated solution was recycled at a fast rate (38.5 L/h, no. 7 in Fig. 1) to aerate and to maintain fully mixed conditions and a constant up-flow rate. Ambient air was used for aeration (flow rate 4 L/min) and the aeration system was placed in a separate column connected to the recycle flow line of the FBR (no. 5 in Fig. 1). A rectangular gravity settling tank (no. 3 in Fig. 1) with the capacity of 25 L (τ_s 0.64–0.65 h, depending on the feed flow rate, see Table 2) was used to remove the precipitates from the solution. The retention time of the gravity settler (τ_s) refers to the hydraulic retention time of the solution in the settling tank:

$$\tau_s(\mathrm{h}) = \frac{V_s}{Q_f + Q_r}$$

where V_s = working volume of the settling tank (L), and Q_r = recycling rate (L/h). The recycling rate was maintained constant during the experiments.

2.2. Mixed culture

The acidophilic iron-oxidizing mixed culture was obtained from an FBR long-term fed with 7 g Fe^{2+}/L and the above described mineral salts medium at pH 0.9. The inoculum was from previous FBR experiments with enrichment cultures that were originally derived from drainage water and sludge samples from the Pyhäsalmi mine, Finland [4,20,22]. The culture was previously found to tolerate elevated iron concentrations and low pH values [22]. The microbial community was monitored by using denaturing gradient gel electrophoresis (DGGE) of PCR-amplified partial 16S rRNA genes as previously described [23]. Fragments corresponding to nucleotide positions 341–926 of the *Escherichia coli* 16S rRNA gene sequence were amplified with the forward primer GC-BacV3f (5′-CCT ACG GGA GGC AGC AG-3′) with a GC clamp at the 5′ end and reverse primer 907r (5′-CCG TCA ATT CMT TTG AGT TT-3′). PCR amplification was performed in a Thermocycler T3000 (Biometra, Göttingen, Germany) with the following program: initial denaturation at 95 °C for 5 min followed by 30 cycles of denaturation at 94 °C for 30 s, primer annealing at 50 °C for 1 min and primer extension at 72 °C for 2 min, and final extension at 72 °C for 10 min. DGGE analysis was performed with total DNA extracted from the feed solution and the operating FBR carrier at different time intervals. The DNA purification and sequencing of the purified products was performed by Macrogen (Seoul, South Korea).

For microscopic counts of bacterial cells, bacteria were sampled from the carrier material and in the FBR outlet and stained with 4′-6-diamidino-2-phenylindole for epifluorescence microscopy. The carrier material samples were sonicated five times for 1 min to detach the carrier-bound cells [4]. Cells were enumerated from 20 microscopic fields for each sample. Activated carbon dry weight was determined by drying the samples at 40 °C for 4 days.

2.3. Analyses

Samples were filtered through a 0.45 μm polysulfone membrane filter (Whatman, Kent, UK) and diluted with 0.7 M HNO_3. The Fe^{2+} concentration was determined colorimetrically (Shimadzu UV 1601 spectrophotometer, Shimadzu, Kyoto, Japan) with ortho-phenanthroline according to modified 3500-Fe method [24]. The iron oxidation performance of the bioprocess can be evaluated by comparing the flow of ferrous iron with the feed solution into the system and with the final effluent out from the system. In this study, the ferrous iron concentrations in the FBR outlet were taken as estimates for the ferrous iron concentrations in the final system effluent (no. 6 in Fig. 1) because the concentrations in the final system effluent were not systematically measured. FBR approaches nearly fully mixed conditions, and the recycling rate was very high compared to the flow rate of the feed solution, and thus the iron concentrations in the final system effluent were essentially the same as the concentrations for the FBR outlet reported here and used for the calculations. As customary for FBR based processes [4,25,26], the fluidized-bed volume was taken as the reference volume when estimating the substrate oxidation rate (R_{FBR}). The rate was calculated as the difference of the Fe^{2+} concentration in the feed solution and in the FBR outlet for the fluidized-bed volume for a given feed rate:

$$R_{FBR}(\mathrm{g/L\,h}) = \frac{Fe^{2+}_{in}Q_f - Fe^{2+}_{out}Q_e}{V_{FBR}} = \frac{Fe^{2+}_{in} - Fe^{2+}_{out}}{\tau_{FBR}}$$

where $Fe^{2+}_{in} = Fe^{2+}$ concentration in the feed (g/L), $Fe^{2+}_{out} = Fe^{2+}$ concentration in the FBR outlet (g/L), and Q_e = flow rate of the final system effluent (L/h) = Q_f. The iron oxidation performance of the overall process is strongly dependent on the capacity of the FBR to retain high level of active iron-oxidizing bacteria. However, the iron oxidation continued in the settling tank and thus for comparison the iron oxidation rate was also calculated with the total volume of the reactor system as the reference flow:

$$R_{tot}(\mathrm{g/L\,h}) = \frac{Fe^{2+}_{in}Q_f - Fe^{2+}_{out}Q_e}{V_{tot}}$$

where V_{tot} = total volume of the reactor system (26 L).

Iron oxidation efficiency of the process was calculated as follows:

$$\text{Iron oxidation efficiency} = \frac{Fe^{2+}_{in} - Fe^{2+}_{out}}{Fe^{2+}_{in}}100\%$$

The pH and dissolved oxygen (DO) were measured using a WTW pH 330i pH meter and a WTW OXI96 dissolved oxygen meter (WTW, Weilheim, Germany), respectively. Oxygen transfer rate (OTR) was calculated from the stoichiometric O_2 requirement for biological Fe^{2+} oxidation ($4Fe^{2+} + 4H^+ + O_2 \rightarrow 4Fe^{3+} + 2H_2O$) as g O_2/L h. Redox potential was measured using Platin Electrode BlueLine 31 Rx (Schott, Mainz, Germany) with Ag/AgCl as the reference electrode. Total suspended solid (TSS) concentration in the settling tank effluent was determined by filtering a 100 mL sample and drying the filter in an oven at 105 °C. Total dissolved iron concentration was determined by using atomic absorption spectrophotometry (PerkinElmer 1100, Waltham, MA, USA). Similarly as with the ferrous iron concentrations, the total dissolved iron concentrations in the FBR outlet were taken as estimates for the total dissolved iron concentrations in the final system effluent, and the rate and efficiency of iron precipitation in the reactor system were calculated as follows:

$$\text{Iron precipitation rate} = \frac{Fe_{tot,in}Q_f - Fe_{tot,out}Q_e}{V_{tot}}$$

and

$$\text{Iron precipitation efficiency} = \frac{Fe_{tot,in} - Fe_{tot,out}}{Fe_{tot,in}}100\%$$

where $Fe_{tot,in}$ = total dissolved iron concentration in the feed (g/L), and $Fe_{tot,out}$ = total dissolved iron concentration in the FBR outlet (g/L).

Settling characteristics of the sludge produced in the reactor were determined from a uniform suspension of a known solids concentration. The volume occupied by 100 mL sludge after 30 min settling was measured with a measuring cylinder. The sludge volume index (SVI), i.e., the volume in mL occupied by 1 g of a suspension after 30 min settling, was determined. The suspended solid concentration of a well mixed sample was determined after drying the samples at 105 °C for 4 h [24].

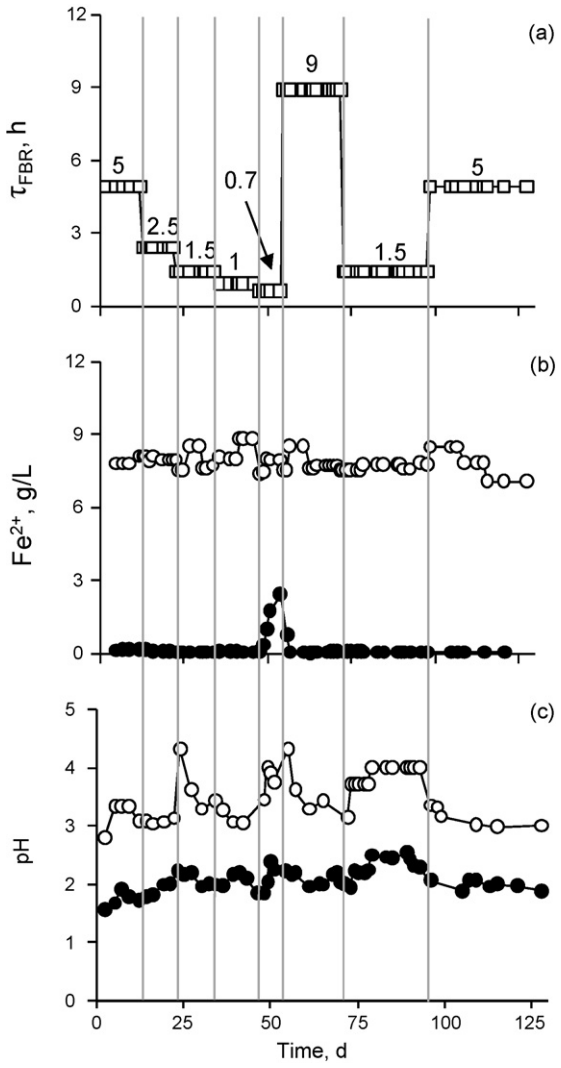

Fig. 2. FBR performance at various τ_{FBR} values over time. (a) τ_{FBR}, (b) Fe^{2+} concentration (feed: ○, FBR outlet: ●), (c) pH (feed: ○, FBR outlet: ●) in the FBR system operated at five different τ_{FBR} values (0.7–5 h). τ_{FBR} of 9 h was maintained after the τ_{FBR} of 0.7 to recover the performance of the reactor.

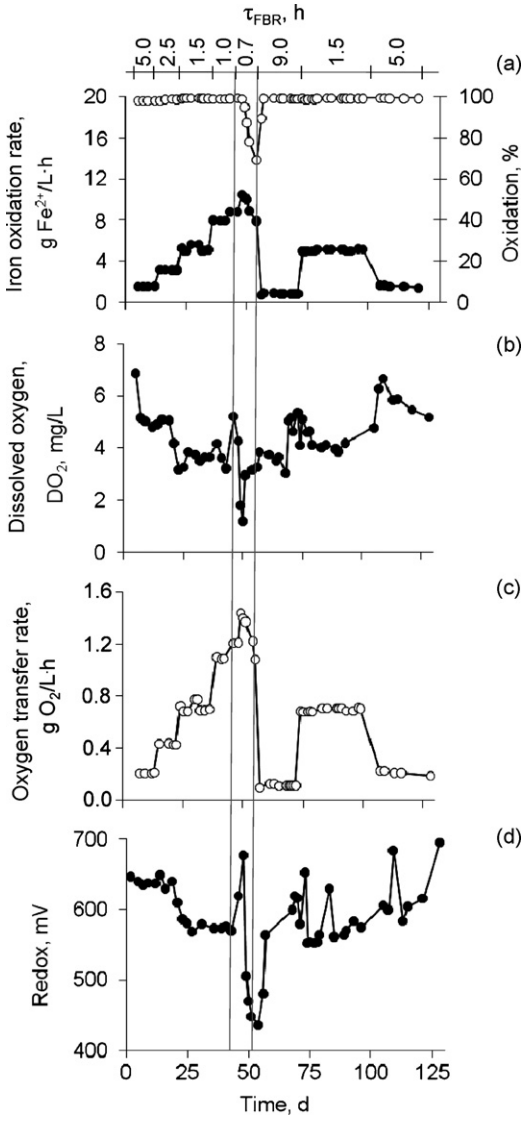

Fig. 3. Changes in FBR performance parameters over time. (a) Iron oxidation rate, R_{FBR} (●: g Fe^{2+}/L h) and efficiency (○: %), (b) dissolved oxygen (DO_2), (c) oxygen transfer rate (g O_2/L h), (d) redox potential.

3. Results and discussion

3.1. Effect of loading rate on iron oxidation

The effect of retention time (τ_{FBR}) on iron oxidation in barren heap leaching solution was studied over a total time course of 145 days (Figs. 2 and 3). The FBR was operated at five different τ_{FBR} values (0.7–5 h) as shown in Fig. 2a. The FBR was first operated at τ_{FBR} of 5 h and then the τ_{FBR} was decreased stepwise to 0.7 h. The FBR was operated for approximately 10 days at each τ_{FBR} before decreasing the τ_{FBR} to 0.7 h. During the periods between τ_{FBR} of 5 and 1 h (days 0–50), the FBR performance was independent of the τ_{FBR} and loading rate. Thereafter, the ferrous iron concentration in the FBR outlet sharply increased from 65 to 2500 mg Fe^{2+}/L at τ_{FBR} of 0.7 h (Fig. 2b) indicating overloading. To recover the FBR steady state conditions, the τ_{FBR} was increased to 9 h and performance of the FBR swiftly improved during this period (days 55–72). In order to determine the stability of the performance, the FBR was operated for a longer period at two different τ_{FBR} levels, 1.5 and 5 h. Ferrous iron was almost completely oxidized in the FBR during all steps except for the τ_{FBR} of 0.7 h, which involved overloading of ferrous iron, although the conversion rate was still high.

Fig. 3 shows the Fe^{2+} oxidation rate (R_{FBR}) and efficiency, DO concentration of the FBR outlet, oxygen transfer rate and redox potential plotted as a function of time. At loading rates below 10 g Fe^{2+}/L h, i.e., above τ_{FBR} of 1 h the Fe^{2+} conversion was almost independent of the loading rate (τ_{FBR}) and remained above 98%. The efficiency of iron oxidation did not change and iron was almost completely oxidized above τ_{FBR} of 0.7 h. At $\tau_{FBR} < 1$ h, the oxidation efficiency decreased due to the oxygen mass transfer limitation. During this period, the DO levels swiftly decreased from around 4–0.7 mg O_2/L. Oxygen mass transfer limitation caused the ferrous iron conversion to decrease. The average conversion during the experiment with τ_{FBR} 0.7 h was 86% and involved a minimum value of 65%. Previously, Kinnunen and Puhakka [4] used a gas mixture containing 99.5% O_2 and 0.5% CO_2 in a ferrous oxidizing FBR to determine whether DO is a rate limiting factor. They observed extremely high oxidation rates with the gas mixture at lower τ_{FBR} values, and concluded that O_2 became the rate limiting factor at low τ_{FBR} values in ferrous iron-oxidizing FBR at acidic pH. Ebrahimi et al. [18] reported that the maximum Fe^{2+} oxidation rate

corresponded to an oxygen transfer rate of 1.7 g O_2/L h in an airlift reactor. In this study, the maximum momentary R_{FBR} was 10.3 g Fe^{2+}/L h and thus the maximum oxygen transfer rate was 1.5 g O_2/L h. The maximum average stable R_{FBR}, 8.2 g Fe^{2+}/L h, was obtained at τ_{FBR} of 1 h. During the longer experimental periods, the R_{FBR} values were 5.1 and 1.6 g Fe^{2+}/L h at τ_{FBR} values of 1.5 and 5 h, respectively. The average iron oxidation rates when taking the total volume of the reactor system as the reference volume (R_{tot}) are summarized in Table 2. The R_{tot} values were around 70 and 20 mg Fe^{2+}/L h at τ_{FBR} values of 1.5 and 5 h, respectively. The dissolved iron concentrations in the final system effluent (no. 6 in Fig. 1) were not systematically measured. However, as the recycled solution also contained iron-oxidizing bacteria, iron oxidation continued in the settling tank. Thus the Fe^{2+} concentrations in the final system effluent were even smaller than the measured concentrations in the FBR outlet. The iron oxidation performance of the reactor system was, therefore, slightly better than reported on the basis of the FBR measurements.

3.2. Effect of loading rate on iron precipitation

The pH values of the feed and FBR outlet were 3.5 ± 0.4 and 2.0 ± 0.2, respectively, and were rather constant during the experiments although they were not controlled (Fig. 2c). In the FBR system, there are two competing reactions involving the hydrogen ion. The biological oxidation of Fe^{2+} iron in the FBR ($4Fe^{2+} + 4H^+ + O_2 \rightarrow 4Fe^{3+} + 2H_2O$) is an acid consuming reaction, whereas iron precipitation as jarosite is an acid producing reaction ($3Fe^{3+} + X^+ + 2HSO_4^- + 6H_2O \rightarrow XFe_3(SO_4)_2(OH)_6 + 8H^+$, X = Na, K, H_3O or NH_4). The pH of the FBR outlet was lower than that of feed solution in the experiments, which resulted from partial iron precipitation as jarosites, confirmed by unpublished X-ray diffraction analysis, in the reactor system. Jarosite precipitation also serves to remove sulfate from the solution, another important control parameter.

In this FBR system, a high-rate effluent recycle was used for aeration and for maintaining fully mixed conditions and a constant up-flow rate. Accordingly, the pH of the FBR outlet was the same as that of the solution in the gravity settler. Under these conditions (pH 2), precipitate formation in the reactor system was limited, being at maximum below 30 mg Fe^{3+}/L h (Fig. 4a) and corresponding to a maximum precipitation of 40–50% (Fig. 4b). For the most part, Fe^{3+} precipitation occurred in the settling tank and thus the τ_s of the settling tank has an effect on the precipitation efficiency. The pH, temperature and ionic composition of the solution also strongly affect the efficiency of Fe(III) precipitation. These effects were not, however, explored in this study.

During the longer experimental periods, the percentage of iron removed in the gravity settler was stable with the values of 28–45% and 34–43% at τ_{FBR} values of 1.5 h (days 73–98) and 5 h (days 99–128), respectively (Fig. 4b). Fe^{3+} precipitation started in the FBR and continued in the settling tank. Therefore, the concentrations of dissolved iron in the recycled solution were even smaller than the measured concentrations in the FBR. The performance of Fe^{3+} precipitation of the entire reactor system was actually slightly better than assessed on the basis of measurements in the FBR.

The performance of the integrated reactor system at different τ_{FBR} values is summarized in Table 2. The rates and efficiencies are presented as average values over the experimental period. The two longer-term experiments (τ_{FBR} values 1.5 and 5 h) are the most representative of the stability and performance of the overall process. The concurrent Fe^{2+} oxidation and Fe^{3+} precipitation were maximized at τ_{FBR} of 1.5 h, with Fe^{2+} oxidation rate (R_{FBR}) of 5.1 g Fe^{2+}/L h (R_{tot} of 66 mg Fe^{2+}/L h) and Fe^{3+} precipitation rate of 25 mg Fe^{3+}/L h (37% iron removal). The relative amount of Fe^{3+} precipitated was within the same range of 37–39% at τ_{FBR} values

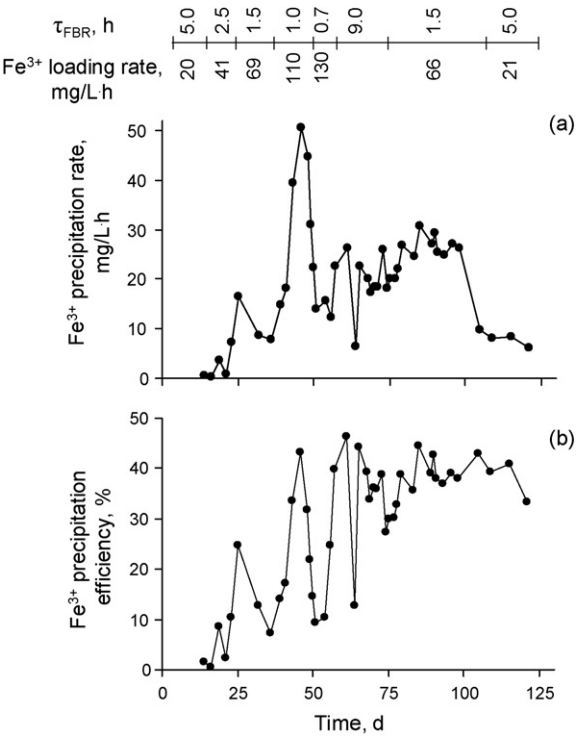

Fig. 4. Precipitation of iron in the gravity settler at different τ_{FBR} runs in FBR. (a) Fe^{3+} precipitation rate, (b) Fe^{3+} precipitation efficiency. Precipitation efficiency is calculated as % Fe^{3+} precipitated from the total amount of Fe^{2+} in the feed.

1.5 and 5 h, indicating that the precipitation and settling process had sufficient capacity for sludge formation and sedimentation and thus partial iron removal from the solution. The τ_s of the settling tank was 0.64–0.65 h depending on the feed flow rate (τ_{FBR}). The experiments demonstrated an association between Fe^{2+} oxidation rate (and thus the loading rate of Fe^{3+} to the settling tank) and Fe^{3+} precipitation rate, indicating that the settling tank provided proper hydraulic conditions for sludge precipitation and settling over long-term operation. The solids were not continuously removed from the settling tank. The SVI of the solids was between 3 and 15 mL/g indicating good settling properties. The good settling properties were also seen from the relatively low TSS values (250 ± 50 mg/L throughout the experiment) of the settling tank effluent. Optimization of the gravity settling process was not undertaken in this study but needs attention because the hydraulic conditions are extremely important for stability, crystallinity and crystallite growth of Fe(III) precipitates. Thus further research is required for optimizing the gravity settler design and for determining properties of Fe(III) precipitates and options for sludge disposal.

3.3. Comparison of the reactor performance to other reactor configurations

The iron oxidation rates for the FBR were higher than values previously reported for most other types of bioreactors. Higher oxidation rates have only been reported for packed-bed bioreactors (Table 1). However, the rate comparison with literature data is somewhat arbitrary, as the volume bases in the calculations often remains unspecified. In the present study, the maximum average iron oxidation rate was 8.2 g Fe^{2+}/L h, and the percentage of iron removed in the gravity settler was 20–50%. Comparative evaluation of the iron removal performance with previous studies is not possible because (i) only a very limited amount of information on

coupled iron biooxidation and precipitation/removal processes is available in the literature, and (ii) sufficient technical and biological details have not been disclosed in previous publications.

Compared to other reactor configurations, an important advantage of the integrated process consisting of a fluidized-bed reactor and a gravity settler developed in this study is the concurrent high-rate iron oxidation and partial precipitative iron removal. Some immobilized cell bioreactor types for iron oxidation have previously been reported to suffer the drawbacks of overgrowth of the cells and extensive precipitation of ferric iron within the carrier matrix, causing strong diffusional resistance against the transfer of nutrients and eventually blockage (Table 1; [19]). With the integrated process presented in this study these drawbacks are virtually non-existent. The fully mixed conditions and constant up-flow rate of the FBR result in efficient mass transfer providing sufficient oxygen supply although some Fe(III) precipitation also occurred in the FBR. Blockage of the carrier matrix was not observed. In previous studies conducted with similar types of FBRs, a jarosite precipitate layer developed during operation on the surface and top of the activated carbon support material and played a beneficial and significant role in retaining active iron oxidizers [4,20]. Ferric iron precipitation is beneficial to the leach circuit because partial removal of iron from regenerated leach liquors prevents iron accumulation in the overall leaching process. The process developed in this study also has high bacterial biomass concentration (in the range of 10^9 cells/g carrier material and 10^7–10^8 cells/mL FBR outlet), which results in high iron oxidation rates and good response to shock loading. The solution treated in this study was from a pilot scale bioleach plant. This was barren solution retrieved after the recovery of valuable metals. The iron in solution was in a completely reduced state, suggesting extensive reduction of ferric iron in the preceding stages of the leach circuit. Bacterial load, if any, in the input solution was of minor importance because the FBR could retain highly active biomass in the matrix.

3.4. Microbial community

PCR-DGGE followed by partial sequencing of 16S rRNA gene showed that the bacterial community of the FBR operated at different τ_{FBR} values was a mixture of *Leptospirillum ferriphilum* and a strain unofficially named "*Ferrimicrobium acidiphilum*" throughout the experiments. "*Ferrimicrobium acidiphilum*" has not been formally characterized but has been found in several mine drainage environments [27–29]. Fig. 5 shows the DGGE profiles of the feed solution and of the carrier material samples taken from the FBR at an early part (day 22) and at the final part of the experiments (day 116). Bands shown in Fig. 5 were excised from the DGGE gel and amplified by PCR and the nucleotide sequences were determined. Bands 1 and 2 showed 99% similarity to *Acidithiobacillus ferrooxidans*, fragments 3–5 and 8 showed 98–99% similarity to *L. ferriphilum* and fragments 6–7 and 9 showed 98–99% similarity to "*Ferrimicrobium acidiphilum*" (Fig. 5 and Table 3). Thus several different bacterial phylotypes were detected in the samples. *A. ferrooxidans* was detected in the barren feed solution obtained from the bioleaching of the multimetal sulfide ore, but this species was not competitive under the experimental conditions since it was never detected in samples from the FBR carrier material. *L. ferriphilum* and "*Ferrimicrobium acidiphilum*" clearly dominated in the microbial community throughout the experiments although the system was continuously supplemented with a mixed community of bioleaching organisms associated with the barren leaching solution. High ferric/ferrous ratios, low pH values [30,4,31] and temperatures above 20 °C [32] have previously been suggested to select for *Leptospirillum* spp. in bioleaching processes, and a combination of experimental conditions also appeared to favor *L. ferriphilum* in this study.

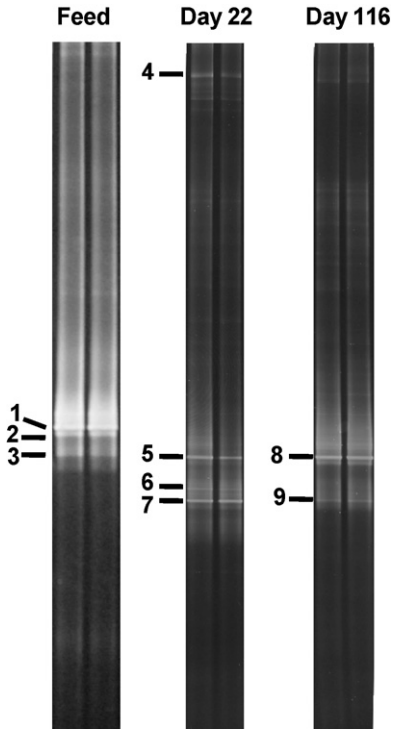

Fig. 5. DGGE profiles (30–70% denaturing gradient) of PCR-amplified partial 16S rRNA genes derived from the DNA extraction of the feed solution and fluidized-bed reactor carrier material (days 22 and 116).

Table 3
DGGE bands and the closest matches of microorganisms.

Band	Accession number	Examples of closest matches	% Similarity
1	FJ587987	*Acidithiobacillus ferrooxidans* FJ157225.1, FJ164046.1, DQ529310.1	99
2	FJ587988	*Acidithiobacillus ferrooxidans* FJ157225.1, FJ164046.1, DQ529310.1	99
3	FJ587989	*Leptospirillum ferriphilum* EU733647.1, EU159264.1, DQ665909.1	98
4	FJ587990	*Leptospirillum ferriphilum* EU733647.1, DQ665909.1, DQ665868.1	99
5	FJ587991	*Leptospirillum ferriphilum* EU733647.1, EU159264.1, EF025342.1	99
6	FJ587992	*"Ferromicrobium acidiphilum"* AJ517364.1, AJ517363.1	98
7	FJ587993	*"Ferromicrobium acidiphilum"* AJ517364.1, AJ517363.1	99
8	FJ587994	*Leptospirillum ferriphilum* EU733647.1, EU159264.1, DQ665868.1	99
9	FJ587995	*"Ferromicrobium acidiphilum"* AJ517364.1, AJ517363.1	99

4. Conclusions

This study demonstrates iron oxidation and partial precipitation in an FBR based reactor system at τ_{FBR} values between 5 and 0.7 h in a barren heap leaching solution with the following conclusions:

1. With air aeration and at loading rates below 10 g Fe^{2+}/L h (τ_{FBR} of 1 h), 98–99% of the Fe^{2+} in the barren heap leaching solution was oxidized in the FBR. The optimal Fe^{2+} oxidation performance with 99% oxidation efficiency and average oxidation rate (R_{FBR})

of 8.2 g Fe^{2+}/L h was achieved at τ_{FBR} of 1 h, which corresponds to the ferrous iron loading rate of 8.3 g Fe^{2+}/L h and oxygen mass transfer rate of 1.2 g O_2/L h. Below this τ_{FBR} oxygen mass transfer from gas to liquid limited the iron oxidation rate.
2. The precipitation of ferric iron produced in the FBR varied from 5% to 40% of the total dissolved iron in solution. The concurrent Fe^{2+} oxidation and partial precipitative iron removal was maximized at the τ_{FBR} of 1.5 h, with R_{FBR} of 5.1 g Fe^{2+}/L h and Fe^{3+} precipitation rate of 25 mg Fe^{3+}/L h, which corresponded to 37% iron removal. Gravity settler in the recycle line of the FBR could be used to remove precipitates from the solution.
3. The bacterial community of the FBR operated at different τ_{FBR} values was dominated by *L. ferriphilum* and "*Ferrimicrobium acidiphilum*" present in the original inoculum although the system was continuously supplemented with bioleaching microorganisms associated with the barren leaching solution.

In summary, a bioprocess was developed in this study that integrated efficient high-rate Fe^{2+} oxidation and partial iron precipitation in barren heap leaching solution. This process was based on a low pH FBR with activated carbon matrix for continuous iron oxidation and a gravity settler for precipitative removal of iron and sulfate. The precipitation prevents iron and sulfate accumulation in bioheap leaching process circuits. We have recently used artificial neural network modeling as well as multiple regression models to predict the extent of Fe(III) precipitation as the final outcome of the process performance [33]. These tools are important because of the need to design and manage bioprocesses such as this, in which large amount of parameters affect the performance of the system and the complex relationships between the parameters are otherwise difficult to identify. The integrated process described herein is robust because of high level of biomass retention. The robustness helps this bioprocess withstand transiently adverse operating conditions in heap bioleaching circuits. Characterization of the solid/liquid separation is warranted to provide a basis for sludge handling, stability and disposal options. Further optimization of the process is application-specific as there is considerable variation in the temperature, chemical composition and microbial community of the potential input solutions.

Acknowledgements

We thank two anonymous reviewers for helpful, insightful suggestions. This research was funded by the Talvivaara Mining Company Plc. O.H. Tuovinen acknowledges support from the Finnish Funding Agency for Technology and Innovation (Finland Distinguished Professor Program, 402/06).

Appendix A. Nomenclature

Fe^{2+}_{in}	Fe^{2+} concentration in the feed (g/L)
Fe^{2+}_{out}	Fe^{2+} concentration in the FBR outlet (g/L)
$Fe_{tot,in}$	total dissolved iron concentration in the feed (g/L)
$Fe_{tot,out}$	total dissolved iron concentration in the FBR outlet (g/L)
Q_e	flow rate of the final system effluent (L/h)
Q_f	feed flow rate (L/h)
Q_r	recycling rate (L/h)
R_{FBR}	Fe^{2+} oxidation rate with fluidized-bed volume as the reference volume (g/L h)
R_{tot}	Fe^{2+} oxidation rate with total volume of the reactor system as the reference volume (g/L h)
V_{FBR}	fluidized-bed volume of the FBR (L)
V_s	working volume of the settling tank (L)
V_{tot}	total volume of the reactor system (L)

Greek letters

τ_{FBR}	retention time of the FBR (h)
τ_s	retention time of the gravity settler (h)

References

[1] Watling HR. The bioleaching of sulphide minerals with emphasis on copper sulphides—a review. Hydrometallurgy 2006;84:81–108.
[2] Haddadin H, Dagot C, Fick M. Models of bacterial leaching. Enzyme Microb Technol 1995;17:290–305.
[3] Hansford GS, Vargas T. Chemical and electrochemical basis of bioleaching processes. Hydrometallurgy 2001;59:135–45.
[4] Kinnunen PH-M, Puhakka JA. High-rate ferric sulfate generation by a *Leptospirillum ferriphilum*-dominated biofilm and the role of jarosite in biomass retainment in fluidized-bed bioreactor. Biotechnol Bioeng 2004;85:697–705.
[5] Lacey DT, Lawson F. Kinetics of the liquid phase oxidation of acid ferrous sulphate by the bacterium *Thiobacillus ferrooxidans*. Biotechnol Bioeng 1970;12:29–50.
[6] Grishin SI, Tuovinen OH. Fast kinetics of Fe^{2+} oxidation in packed-bed reactors. Appl Environ Microbiol 1988;54:3092–100.
[7] Mazuelos A, Carranza F, Palencia I, Romero R. High efficiency reactor for biooxidation of ferrous iron. Hydrometallurgy 2000;58:269–75.
[8] Ginsburg MA, Penev K, Karamanev D. Immobilization and ferrous iron biooxidation studies of a *Leptospirillum* sp. mixed-cell culture. Miner Eng 2009;22:140–8.
[9] Diz HR, Novak JT. Modeling biooxidation of iron in packed-bed reactor. J Environ Eng 1999;125:109–16.
[10] Gomez JM, Cantero D. Kinetic study of biological ferrous sulphate oxidation by iron-oxidising bacteria in continuous stirred tank and packed bed bioreactors. Process Biochem 2003;38:867–75.
[11] Long Z, Huang Y, Cai Z, Cong W, Ouyand F. Biooxidation of ferrous iron by immobilized *Acidithiobacillus ferrooxidans* in poly(vinyl alcohol) cryogel carriers. Biotechnol Lett 2003;25:245–9.
[12] Nemati M, Webb C. Effect of ferrous iron concentration on the catalytic activity of immobilized cells of *Thiobacillus ferrooxidans*. Appl Microbiol Biotechnol 1996;46:250–5.
[13] Wood TA, Murray KR, Burgess JG. Ferrous sulphate oxidation using *Thiobacillus ferrooxidans* cells immobilised on sand for the purpose of treating acid mine-drainage. Appl Microbiol Biotechnol 2001;56:560–5.
[14] Nakamura K, Noike T, Matsumoto J. Effect of operation conditions on biological Fe^{2+} oxidation with rotating biological contactors. Water Res 1986;20:73–7.
[15] Nikolov L, Mehochev D, Dimitrov D. Continuous bacterial ferrous iron oxidation by *Thiobacillus ferrooxidans* in rotating biological contactors. Biotechnol Lett 1986;8:707–10.
[16] Armentia H, Webb C. Ferrous sulphate oxidation using *Thiobacillus ferrooxidans* cells immobilized in polyurethane foam support particles. Appl Microbiol Biotechnol 1992;36:697–700.
[17] Jensen AB, Webb C. A trickle bed reactor for ferrous sulphate oxidation using *Thiobacillus ferrooxidans*. Biotechnol Techn 1994;8:87–92.
[18] Ebrahimi S, Fernández Morales FJ, Kleerebezem R, Heijnen JJ, van Loosdrecht MCM. High-rate acidophilic ferrous iron oxidation in a biofilm airlift reactor and the role of the carrier. Biotechnol Bioeng 2005;90:462–72.
[19] Nemati M, Harrison STL, Hansford GS, Webb C. Biological oxidation of ferrous sulphate by *Thiobacillus ferrooxidans*: a review on the kinetic aspects. Biochem Eng J 1998;1:171–90.
[20] van der Meer T, Kinnunen PH-M, Kaksonen AH, Puhakka AJ. Effect of fluidized-bed carrier material on biological ferric sulphate generation. Miner Eng 2007;20:782–92.
[21] Ozkaya B, Sahinkaya E, Nurmi P, Kaksonen AH, Puhakka JA. Iron oxidation and precipitation in a simulated heap leaching solution in a *Leptospirillum ferriphilum* dominated biofilm reactor. Hydrometallurgy 2007;88:67–74.
[22] Kinnunen PH-M, Puhakka JA. High-rate iron oxidation at below pH 1 and at elevated iron and copper concentrations by a *Leptospirillum ferriphilum* dominated biofilm. Process Biochem 2005;40:3536–41.
[23] Özkaya B, Sahinkaya E, Nurmi P, Kaksonen AH, Puhakka JA. Kinetics of iron oxidation by *Leptospirillum ferriphilum* dominated culture at pH below one. Biotechnol Bioeng 2007;97:1121–7.
[24] American Public Health Association. Standard methods for the examination of water and wastewater, 18th ed., Washington, DC: American Public Health Association; 1992.
[25] Buffière P, Moletta R, Fonade C. Continuous operations of a fluidized bed bioreactor for anaerobic digestion: residence time effect on degradation kinetics. Biotechnol Lett 1995;1:833–8.
[26] Rabah FKJ, Dahab MF. Nitrate removal characteristics of high performance fluidized-bed biofilm reactors. Water Res 2004;38:3719–28.

[27] Bacelar-Nicolau P, Johnson DB. Leaching of pyrite by acidophilic heterotrophic iron-oxidizing bacteria in pure and mixed culture. Appl Environ Microbiol 1999;65:585–90.
[28] Bond PL, Smriga SP, Banfield JF. Phylogeny of microorganisms populating a thick, subaerial, predominantly lithotrophic biofilm at an extreme acid mine drainage site. Appl Environ Microbiol 2000;66:3842–9.
[29] Brofft JE, McArthur JV, Shimkets LJ. Recovery of novel bacterial diversity from a forested wetland impacted by reject coal. Environ Microbiol 2002;4:764–9.
[30] Rawlings DE, Tributsch H, Hansford GS. Reasons why '*Leptospirillum*'-like species rather than *Thiobacillus ferrooxidans* are the dominant iron-oxidizing bacteria in many commercial processes for the biooxidation of pyrite and related ores. Microbiology 1999;145:5–13.
[31] Plumb JJ, Muddle R, Franzmann PD. Effect of pH on rates of iron and sulfur oxidation by bioleaching organisms. Miner Eng 2008;21:76–82.
[32] Sand W, Rohde K, Sobotke B, Zenneck C. Evaluation of *Leptospirillum ferrooxidans* for leaching. App Environ Microbiol 1992;58:85–92.
[33] Nurmi P, Özkaya B, Kaksonen AH, Tuovinen OH, Puhakka JA. Predictive modelling of Fe(III) precipitation in iron removal process for bioleaching circuits. Bioprocess Biosyst Eng 2009; doi:10.1007/s00449-009-0346-5, in press.